TRENDS IN SCIENCES 2026; 23(12): 14206
https://doi.org/10.48048/tis.2026.14206 RESEARCH ARTICLE

Synergistic Antibacterial Effect of Quercetin and Cefotaxime on Extended-Spectrum *β*-Lactamase-Producing *Acinetobacter baumannii*

Intu-orn Ayamuang[1], Yothin Teethaisong[2], Santi Watthana[1], Kittipot Sirichaiwetchakoon[3], Benjawan Dunkhunthod[4], Siriporn Suknasang[5], Yupaporn Chaiseha[1] and Griangsak Eumkeb[5,*]

[1]*School of Biology, Institute of Science, Suranaree University of Technology, Nakhon Ratchasima 30000, Thailand*
[2]*Department of Medical Sciences, Faculty of Allied Health Sciences, Burapha University, Chon Buri 20131, Thailand*
[3]*Division of Pharmacology and Biopharmaceutical Sciences, Faculty of Pharmaceutical Sciences, Burapha University, Chonburi 20131, Thailand*
[4]*Thai Traditional Medicine Program, Faculty of Nursing and Allied Health Sciences, Phetchaburi Rajabhat University, Phetchaburi 76000, Thailand*
[5]*School of Preclinical Sciences, Institute of Science, Suranaree University of Technology, Nakhon Ratchasima 30000, Thailand*

([*]Corresponding author's e-mail: griang@g.sut.ac.th)

Received: 27 April 2026, Revised: 8 June 2026, Accepted: 18 June 2026, Published: 1 August 2026

Abstract

Acinetobacter baumannii (*A. baumannii*) is a critical multidrug-resistant pathogen designated by the WHO as a major global health threat, with rising resistance to third-generation cephalosporins and carbapenems severely restricting therapeutic options. This study explores the novel potential of combining conventional antibiotics with plant-derived compounds, focusing on quercetin (QUE), a bioactive flavonoid. We evaluated the synergistic antibacterial activity and mechanisms of cefotaxime (CTX)–QUE combinations against 3 β-lactam-resistant *A. baumannii* strains (DMST 43250, DMST 44689, DMST 45378). All strains exhibited high CTX resistance (MIC 1,024 μg/mL) and harbored the bla_{TEM} gene, consistent with β-lactamase-mediated resistance. Notably, CTX–QUE demonstrated strong synergy (FICI 0.31) against strain DMST 45378, with time kill assays confirming sustained antibacterial activity (≥ 2 $\log_{10}$ CFU/mL reduction compared with QUE alone). Mechanistic analyses revealed significant cytoplasmic membrane disruption, leakage of intracellular DNA/RNA, and marked morphological damage. In addition, QUE inhibited biofilm formation and altered biomolecular profiles, while exhibiting appreciable cytotoxicity in human keratinocytes under *in vitro* conditions. Collectively, these findings highlight the novelty of employing a natural flavonoid to potentiate β-lactam activity and support the promise of plant-derived compounds as adjunctive strategies against WHO critical priority pathogens. Further studies are warranted to validate this combination before clinical application against β-lactam-resistant *A. baumannii.*

Keywords: *Acinetobacter baumannii*, *β*-lactam-resistant, Biofilm inhibition, Cefotaxime, Multidrug resistance, Quercetin, Synergistic activity

Introduction

Nosocomial infections, also called hospital-acquired infections (HAIs), are a group of infections caused by many opportunistic pathogens [1]. The ESKAPE group of opportunistic pathogens, including *Enterococcus faecium*, *Staphylococcus aureus*, *Klebsiella pneumoniae*, *Acinetobacter baumannii*, *Pseudomonas aeruginosa*, and *Enterobacter* spp., known for causing HAIs, exhibits high multidrug resistance, ranging from first-line to last-resort antibiotics [2,3]. Among the pathogens that cause infections, carbapenem-resistant *Acinetobacter*

baumannii (CRAB) has received special attention because it can cause severe infections and develop resistance to multiple drugs [4]. In 2024, the World Health Organization (WHO) categorized 3 priority tiers of antibiotic-resistant bacteria that necessitate research and development of novel antimicrobial agents, including critical, high, and medium priority. CRAB is listed as a critical-priority pathogen [5]. The resistance mechanisms in bacteria have steadily increased against numerous antibiotics. As a result, the development of new therapeutic strategies continues to face significant challenges. A synergistic approach has shown potential in restoring antibacterial activity. This strategy involves combining antimicrobial agents [6] or pairing antibiotics with bioactive compounds such as flavonoids [7,8] as alternative therapies for infections caused by antibiotic-resistant opportunistic pathogens. Such an approach can slow the evolution of bacterial resistance and extend the effectiveness of existing antibiotics.

A. baumannii is a Gram-negative bacterium frequently implicated in ventilator-associated pneumonia, bloodstream infections, wound infections, and urinary tract infections, particularly in intensive care units [9]. It can produce biofilm, which allows it to persist in hospitals for extended periods due to its ability to survive on inanimate surfaces, resist desiccation, and withstand commonly used disinfectants, making it a significant challenge in infection control. Furthermore, the biofilm formation rate in this species is higher than in other species [10,11]. Multidrug-resistant (MDR) *A. baumannii* infections have increasingly disseminated in the last decade worldwide. Recently, this pathogen has exhibited resistance to all *β*-lactams, fluoroquinolones, and aminoglycosides by similar mechanisms to those of *P. aeruginosa* and Enterobacteriaceae [12]. Recently, colistin, sulbactam, and tigecycline still have been used in clinical treatment but there is increasing patient toxicity [13].

Cefotaxime (CTX) is a third-generation cephalosporin administered via intramuscular or intravenous injection and was one of the first drugs in its class to be marketed. It exhibits broad-spectrum activity against *β*-lactamase-producing bacteria, including Enterobacteriaceae, *E. coli*, *Pseudomonas* spp., *N. gonorrhoeae*, *N. meningitidis*, *S. aureus*, *Streptococcus pyogenes*, and *Streptococcus pneumoniae*. CTX is used to treat a variety of infections, such as urinary tract infections, lower respiratory tract infections, meningitis, uncomplicated gonorrhea, skin infections, and pneumonia [14]. In Thailand, according to the 2026 National List of Essential Medicines, CTX remains an alternative treatment for neonatal bacterial infections, primarily to avoid the adverse effects associated with ceftriaxone [15]. Of concern, national antibiogram data indicate that more than 50% of *A. baumannii* isolates from all specimen types remain susceptible to CTX [16], underscoring its continued clinical relevance despite rising antimicrobial resistance. Its mode of action involves binding to penicillin-binding proteins during the transpeptidation step of bacterial cell wall synthesis and interfering with *β*-lactamase activity. Class A, *β*-lactamase enzymes, including TEM, were first identified by a patient named “Temoniera” which is found widely on plasmids of Gram-negative bacteria [17]. CTX has synergistic activity with *Allium sativum* against ceftazidime-resistant *E. coli* from skin and soft tissue infections [18]. Moreover, nanoparticles such as silver and bismuth telluride are conjugated with CTX to enhance antibacterial efficiency against multidrug-resistant bacteria [19,20].

Quercetin (QUE) is a polyphenolic flavonoid renowned for its multifaceted biological activities, including anti-SARS-CoV-2, antioxidant, anti-inflammatory, anticancer, and antimicrobial effects [21-24]. Its antimicrobial action is attributed to several mechanisms: Quercetin can disrupt bacterial cell membranes, leading to increased permeability and leakage of cellular contents, inhibit nucleic acid synthesis, and interfere with energy metabolism. Additionally, quercetin modulates efflux pump activity in bacteria, which can enhance the efficacy of conventional antibiotics against multidrug-resistant strains. QUE has a broad spectrum of antibacterial activity to treat MDR bacterial strains by inhibiting DNA gyrase and topoisomerase IV. It plays an important role in DNA replication in prokaryotes such as *Vibrio harveyi*, *Bacillus subtilis*, *and Mycobacterium* spp. [25,26]. It promotes cell wall disruption and lysis by an expressed inhibitor to inhibit the reaction of fatty acid synthesis in *H. pylori* and interfere with the stability of the cell wall layer and thickness, causing intracellular matrix leak and death in *S. aureus* and *Streptococcus mutants* [27]. In *E. coli*, QUE at MIC 33 μg/mL interrupts the amino acid in the porin structure within

the bacterial cell membrane [28]. Biofilm formation in MRSA, *E. coli*, and *P. aeruginosa* was inhibited by QUE in a concentration dependent manner [29]. Moreover, the synergistic effect of QUE plus amoxicillin antibiotic has an effect against amoxicillin-resistant *Staphylococcus epidermidis* [30]. The studies of QUE against oral and gastrointestinal microbes showed that this compound had strong activity to block *Porphyromonas ginggivalis* and *H. pylori* growth [31,32].

Acinetobacter baumannii is classified by the WHO as a critical priority pathogen due to escalating resistance to β- lactam antibiotics, which severely limits therapeutic options. Natural compounds such as QUE exhibit antibacterial activity, yet their capacity to potentiate β-lactam efficacy remains uncertain. The synergistic interaction between CTX and QUE against β-lactam-resistant *A. baumannii* has not been previously characterized. This study, therefore, investigated CTX-QUE synergy and underlying mechanisms using minimum inhibitory concentration (MIC) assays, checkerboard analysis, time kill curves, PCR detection of resistance genes, evaluation of cell envelope disruption, biomolecular profiling by FTIR, and cytotoxicity testing. Findings underscore the novelty of employing a flavonoid to enhance β-lactam activity and highlight the potential of plant-derived compounds as adjunctive agents in antimicrobial therapy.

Materials and methods

Bacterial strains

Three *A. baumannii* strains (DMST 43250, 44689, and 45378) were purchased from the Ministry of Public Health, Thailand. *E. coli* ATCC 25922 was used as a positive control. All experiments were conducted using standardized bacterial inocula with an initial concentration of 5×10^5 CFU/mL.

Antibiotic and bioactive compounds

CTX, imipenem (IPM), polymyxin B (PMB), and QUE were purchased from Sigma-Aldrich, USA, and Indofine, USA, respectively. Stock solutions (10,240 µg/mL, 10×) were prepared in sterile water for antibiotics or in dimethyl sulfoxide (DMSO) for QUE, and stored at 4 °C until use.

Minimum inhibitory concentrations (MICs)

To determine the antibacterial effect of CTX, IPM, and QUE against 3 strains of *A. baumannii* and *E. coli* (a positive control). The MICs were performed following the Clinical and Laboratory Standards Institute [33]; Liu *et al.* [34]. Briefly, overnight cultures were grown in cation-adjusted Mueller-Hinton broth (CAMHB) at 37 °C, washed, and the absorbance was adjusted to 0.08 - 0.13 at a wavelength of 600 nm (~1×10^8 CFU/mL) by UV-VIS spectrophotometer. Suspensions were diluted to 5×10^5 CFU/mL and inoculated into 96-well plates containing serial dilutions of test agents. Wells that presented no antibacterial agent were determined as positive, and no bacteria in wells were determined as negative controls, respectively. After overnight incubation, bacterial growth was measured by absorbance. The lowest concentration with no visible growth was recorded as the MIC.

Detection of *β*-lactam antibiotic resistance genes in *A. baumannii*

This study used primer sets specifically targeting *β*-lactamase genes, including those from the bla_{ampC} family [35], the bla_{ESBL} family [3], and various *carbapenemase* genes [3]. The primer sequences and concentrations used are detailed in **Tables S1** - **S3**, respectively. Genotypic resistance testing was performed using PCR, following the method by Teethaisong *et al.* [36]. Briefly, DNA was extracted from overnight cultures (5 mL) using the GF-Bacterial DNA Extraction Kit (Vivantis, Malaysia). DNA quality was assessed by a NanoDot microspectrophotometer. PCR was performed in 50 µL reactions containing 200 ng template, 1 µM primers, 25 µL of GoTaq Green Master Mix (Promega, USA), and nuclease-free water. The tube containing DNase-free water in place of template DNA was used as a negative control. Cycling conditions consisted of initial denaturation (95 °C, 5 min), followed by 30 cycles of denaturation, annealing (60 or 64 °C depending on primers), and extension (72 °C, 1 min), with a final extension at 72 °C for 7 min.

Checkerboard assay

The synergistic interaction between CTX and QUE was assessed by checkerboard microdilution. Two-fold serial dilutions of CTX and QUE starting from

the MIC were combined in 96-well plates containing 5×10^5 CFU/mL bacterial inoculum. Then, the reaction was incubated overnight. The interaction was determined as previously described by Bonapace and co-workers' method [37]. The result was calculated by the Fractional Inhibitory Concentration index (FICI) as described by Marques *et al.* [38] following this formula;

$$FICI = FIC(A) + FIC(B) = \frac{\text{Conc. of A in MICs of A + B}}{\text{MIC of A alone}} + \frac{\text{Conc. of B in MICs of A + B}}{\text{MIC of B alone}}$$

The FICI ≤ 0.5 indicates synergy, > 0.5 to < 1.0 denotes partial synergy, 1.0 denotes additive effect, > 1.0 to < 4.0 denotes indifference, and > 4.0 denotes antagonism. The strain with the lowest FICI was selected for further assays.

Time-killing curve determination

Synergistic activity was confirmed by time-kill kinetics. The bacterial strain with the lowest FICI was selected to study the time-kill assay, as previously described by Michael *et al.* [39]. Cultures (5×10^5 CFU/mL) were exposed individually to sub-MIC concentrations of CTX, QUE, or their combination. Viable counts were determined at 0, 1, 2, 4, 6, 8, and 24 h by plating serial dilutions. A ≥ 2 $\log_{10}$ CFU/mL reduction at 24 h for the combination compared with the most active single agent (CTX or QUE) was defined as synergy.

Cytoplasmic membrane (CM) permeability

To monitor total nucleic acids (DNA and RNA) leakage across the bacterial cell using a UV-VIS spectrophotometer at OD_{260}. This method was performed as previously described by Teethaisong *et al.* [40]. Shortly, Bacteria (5×10^5 CFU/mL) were suspended individually in sodium hydroxyethyl piperazineethanesulfonic acid buffer (2.5 mM, pH 7.2) with 100 mM glucose and treated with sub-MIC concentrations of CTX, QUE, or their combination. Nisin was used as a positive control. Supernatants were collected at 0 - 4 h, filtered (0.2 μm), and analyzed. Each condition at a different time point was measured at OD260. All measurements were conducted in triplicate, and data were graphically presented using SigmaPlot version 12.0 software.

Anti-biofilm formation

Biofilm is an extracellular polymeric substance that is challenging to eliminate, including proteins, nucleic acids, and polysaccharides. The effect of anti-biofilm formation was studied following the method of Gopal *et al.* [41]. Bacteria (5×10^5 CFU/mL) were incubated in CAMHB with CTX, QUE, or their combination for 48 h at 37 °C. Subsequently, the wells were washed, stained with 0.4% (w/v) crystal violet for 30 min, rinsed, and air-dried. The stain was solubilized with 95% ethanol, and absorbance at 600 nm was measured. All assays were performed in triplicate to ensure accuracy and reproducibility.

Ultrastructure damage comparison using scanning and transmission electron microscopes (SEM & TEM)

The SEM and TEM were employed to compare the impact of the test compounds on bacterial morphology, as previously described by Teethaisong *et al.* [42]. To evaluate ultrastructural changes, bacteria were incubated separately with sub-MIC concentrations of CTX, QUE, or their combination for 4 h. Cells were harvested, fixed with 2.5% glutaraldehyde in 0.1 M phosphate buffer overnight, and post-fixed with 1% OsO_4. Samples were dehydrated in graded acetone, stained with 3% uranyl acetate, and prepared for SEM (Auriga, Zeiss, Germany). For TEM, these samples were fixed for 15 min using 2% (w/v) uranyl acetate and 0.25% (w/v) lead citrate. Then, the specimens were subsequently observed and captured using a 120 kV electron microscope. Images were acquired randomly to minimize bias.

Comparative biomolecular alterations using Fourier-transform infrared spectroscopy (FTIR)

To determine the effect of QUE and CTX, either alone or in combination, on *A. baumannii* DMST 45378 on biochemical change. The FTIR measurement was performed, and this study followed the previous researchers [30,43,44]. Biochemical alterations were analyzed using synchrotron-based FTIR (Hyperion 2000, Bruker Optics) at beamline 4.1, Synchrotron Light Research Institute, Thailand. Spectra were collected in the 3,000 - 900 cm^{-1} range. Integrated peak areas of lipid (3,000 - 2,800 cm^{-1}), protein (1,800 - 1,400 cm^{-1}),

carbohydrate, and nucleic acid (1,300 - 950 cm^{-1}) regions were calculated. Amide I/II ratios were determined, and second derivative spectra were plotted using OriginPro 9.0 and SigmaPlot 12.0.

Assessment of cytotoxicity in human keratinocyte (HaCaT) cells

The cytotoxic effects and safe dosage ranges of CTX, QUE, and their combination were assessed using HaCaT through the MTT assay. The assay was conducted following methods previously described by Dunkhunthod *et al.* [45]. Briefly, HaCaT cells (CLS Cell Lines Service, Germany) were cultured in Dulbecco's modified Eagle medium (DMEM) with 10% fetal bovine serum, 1% of 100 units of penicillin, and streptomycin (100 µg/mL). Cells were seeded at 1.5×10^4 cells per well in 96-well plates and incubated overnight. Varying concentrations of CTX, QUE, and combinations were applied for 24 h, followed by incubation with MTT (0.5 mg/mL) for 4 h. Formazan crystals were solubilized with 100% DMSO, and absorbance was measured at 540 nm. Cell viability was calculated relative to untreated controls. All assays were performed in triplicate to ensure accuracy and viability.

Statistical analysis

All experiments were performed in triplicate. Data from permeability, biofilm, and FTIR assays were analyzed by 1-way ANOVA with Tukey's HSD post-hoc test ($p < 0.05$). Cytotoxicity was analyzed by ANOVA with LSD post-hoc test ($p < 0.01$). Analyses were performed with SPSS v26 (IBM, USA).

Results and discussion

MICs, MBCs, and checkerboard determination

The results indicated that *A. baumannii* strains (DMST 43250, 44689 and 45378) displayed resistance to CTX, with the MICs at 1,024 µg/mL, while the reference strain of *E. coli* ATCC 25922 exhibited susceptibility to CTX with a MIC of 0.12 µg/mL [33]. Similarly to IPM, all bacterial strains were resistant to IPM with MICs of 32 - 64 µg/mL, while the reference strain of *E. coli* ATCC 25922 exhibited susceptibility with a MIC of 0.25 µg/mL. QUE demonstrated high MICs (1,024 µg/mL) against all 3 *A. baumannii* strains. The checkerboard assay revealed the synergistic activity of QUE plus CTX against *A. baumannii,* with the FICI between 0.31 and 0.625 (synergism to partial synergism), in which CTX concentrations were greatly reduced compared to using CTX alone (**Table 1**).

Table 1 Minimum inhibitory concentrations (MICs), Fraction Inhibitory Concentrations (FICs), and FIC index (FICI) of cefotaxime (CTX), imipenem (IPM), and quercetin (QUE) against *A. baumannii* spp.

Bacterial Strains	MIC (µg/mL)			FIC CTX + QUE (µg/mL)	FIC index	Interpretation
	CTX	IPM	QUE			
A. baumannii DMST 45378	1024^{R}	32^{R}	$1024^{N/D}$	256 + 64	0.31	Synergy
A. baumannii DMST 44689	1024^{R}	64^{R}	$1024^{N/D}$	256 + 256	0.5	Synergy
A. baumannii DMST 43250	1024^{R}	64^{R}	$1024^{N/D}$	512 + 128	0.625	Partial synergism
E. coli ATCC 25922*	0.12^{S}	0.25^{S}	$1024^{N/D}$	0.12 + 32	1.125	Indifference

^{S} = Susceptible; ^{R} = Resistant; $^{N/D}$, not determined; * = A quality control strain for *Acinetobacter* spp. Susceptibility profiles were interpreted based on CLSI guidelines.

The emergence of MDR *A. baumannii* presents major healthcare challenges worldwide, limiting treatment options and complicating infection control [6,46]. The present study evaluated the antibacterial property and investigated the mechanism of action of CTX, a *β*-lactam antibiotic, combined with QUE, a natural flavonoid, against cefotaxime-resistant *A. baumannii* strains.

Currently, third-generation cephalosporins are still used for treating *A. baumannii* infections [15,16,47]. In this study, initial susceptibility testing revealed high resistance to CTX (MIC = 1,024 µg/mL) in strains DMST 43250, 44689, and 45378, which is consistent

with *β*-lactamase–mediated hydrolysis [6,48]. QUE alone also exhibited antibacterial activity, with an MIC of 1,024 µg/mL. Notably, in strain DMST 45378, the combination of CTX and QUE reduced the MIC of CTX by 4-fold and that of QUE by 16-fold, resulting in a synergistic FIC index of 0.31. This finding is consistent with previous reports suggesting that flavonoids can enhance antibacterial activity through *β*-lactamase inhibition or by increasing membrane permeability [7,49]. Furthermore, earlier studies have shown that cefoperazone-sulbactam achieves higher clinical cure rates when used in combination with other antibiotics, such as carbapenems, polymyxins, or tigecycline/minocycline, compared with monotherapy in *A. baumannii* infections [47]. These findings are restricted to the 3 β-lactam-resistant *A. baumannii* strains examined and therefore cannot be generalized to all β-lactam-resistant *A. baumannii* isolates.

Detection of *β-lactamase*-specific genes by PCR

This study utilized PCR methodology to target 3 significant *β*-lactamase gene families, including bla_{ampC}, bla_{ESBL}, and *carbapenemase* family genes, in *Acinetobacter baumannii* species. The PCR analysis revealed that all tested isolates (*A. baumannii* DMST 43250, 44689, and 45378) contained the ESBLs (bla_{TEM}) gene, while none exhibited the presence of bla_{ampC} and *carbapenemase* family genes (**Figure 1**).

PCR analysis confirmed acquired *β*-lactam resistance genes. Among bla_{ampC}, bla_{ESBL}, and *carbapenemase* families, only bla_{TEM} (bla_{ESBL}) was detected. These results align with MIC data and prior studies showing TEM variants confer resistance to penicillins, cephalosporins, and monobactams [50]. Paterson and Bonomo [51] emphasized the clinical significance of ESBLs, particularly bla_{TEM} and bla_{SHV}, in Gram-negative bacteria, with frequent detection in Enterobacteriaceae and occasional occurrence in *Pseudomonas* spp. and *A. baumannii*. The bla_{TEM} is highly transmissible via mobile elements [52]. Detection of only bla_{TEM} confirms the presence of a β-lactamase gene, serving as preliminary screening. As only selected resistance genes were assessed, additional mechanisms may contribute to the observed cefotaxime and imipenem resistance, underscoring the need for further investigation.

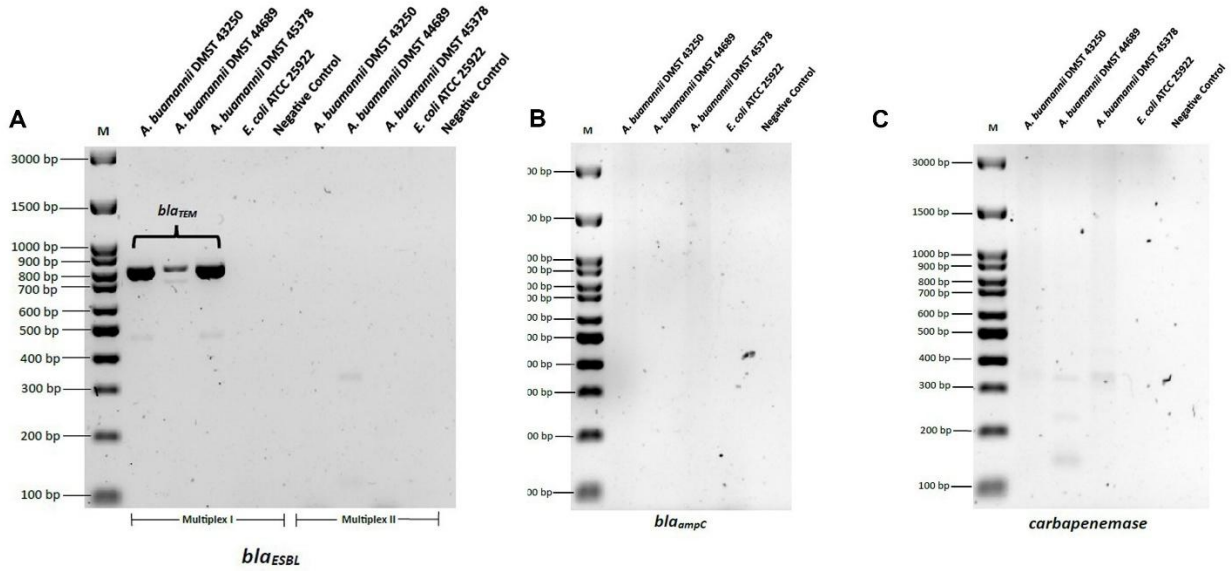


Figure 1 PCR for the identification of *β*-lactamase gene families in 3 strains of *A. baumannii*. bla_{ESBL} family gene (A); bla_{ampC} (B); *carbapenemase* (C). (M) DNA ladder. *E. coli* ATCC 25922 was used as the quality control strain for assessing the susceptibility profiles of *Acinetobacter* spp. following CLSI guidelines.

Time-killing curve

The time-killing curve (**Figure 2**) illustrates the time-dependent antibacterial activity of CTX and QUE, both alone and combined, against *A. baumannii* DMST 45378. Untreated bacterial cells (CON) rapidly grew over 24 h. CTX alone at 512 µg/mL initially reduced

bacterial counts, but regrowth occurred after 8 h, indicating incomplete inhibition. QUE alone at 512 μg/mL demonstrated limited inhibition throughout the experiment. Notably, the combination treatment (CTX at 256 μg/mL plus QUE at 64 μg/mL) showed a significant and sustained reduction in bacterial counts ≥ 2 $\log_{10}$ CFU/mL compared with treatment using QUE alone over 24 h, without evidence of bacterial regrowth, highlighting strong synergistic antibacterial activity (**Figure 2**).

Time-kill assays supported sustained antibacterial efficacy. Monotherapies caused temporary suppression followed by regrowth, while combination therapy achieved ≥ 2 $\log_{10}$ reduction in viable counts with no regrowth at 24 h. This effect likely stems from enhanced CTX accumulation via QUE-induced membrane disruption [7,30].

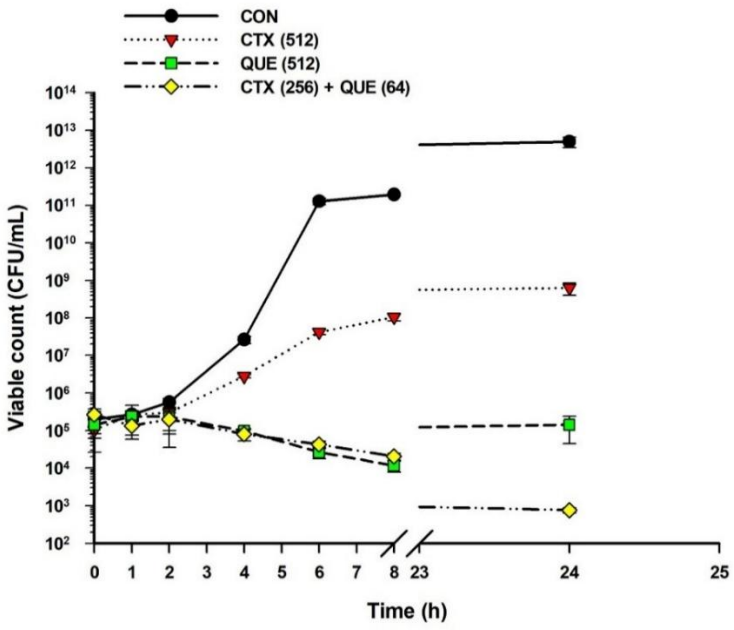


Figure 2 Time-kinetic inhibition of *A. baumannii* DMST 45378 after exposure to quercetin (QUE) alone and in combination with cefotaxime (CTX) at different time points. CON; untreated cells, CTX (512); cefotaxime at 512 μg/mL, QUE (512); quercetin at 512 μg/mL, and CTX (256) + QUE (64); cefotaxime at 256 μg/mL plus quercetin at 64 μg/mL. The values plotted are the means of 3 observations (n = 3), and the vertical bars indicate standard deviation (S.D.).

CM permeability

The lowest FIC index strain was chosen for further investigation of the antibacterial mode of action. **Figure 3** presents data on the leakage of intracellular constituents (such as DNA and RNA) from *A. baumannii* DMST 45378 after exposure to CTX, QUE, and their combination. PMB was used as a positive control. The untreated control cells (CON) showed minimal leakage throughout the experiment, reflecting intact cell integrity. QUE and the combination significantly increased leakage from 0.5 h compared to other treatments ($p < 0.05$). CTX alone (512 μg/mL) and PMB alone (2 μg/mL) induced moderate increases in leakage, with PMB exhibiting greater leakage effects than CTX alone. In addition, the combination of CTX (128 μg/mL) and QUE (32 μg/mL) resulted in a significant increase in intracellular constituent leakage compared to other treatments from 1 h through to the end of the experiment ($p < 0.05$), surpassing the effects observed with each agent individually and approaching the stronger effect than PMB (**Figure 3**).

CM permeability testing showed that CTX or QUE alone caused moderate leakage of intracellular constituents, whereas their combination produced significantly greater leakage, even exceeding PMB [53]. QUE's disruption of membrane integrity appears to facilitate CTX penetration, resulting in extensive cellular breakdown [7,49]. Such synergistic membrane damage aligns with prior reports of flavonoid-antibiotic combinations [30,54].

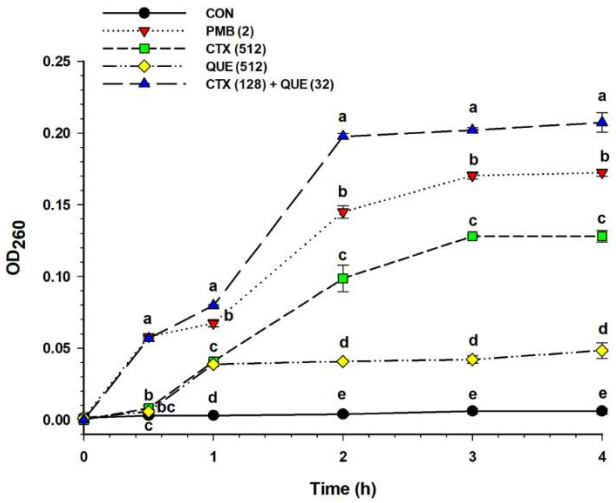


Figure 3 The effect of CTX, QUE alone, and combined on intracellular constituents (DNA, RNA, enzyme, and ATP) leakage of *A. baumannii* DMST 45378. CON; untreated control, PMB (2); polymyxin B at 2 µg/mL, CTX (512); cefotaxime at 512 µg/mL, QUE (512); quercetin at 512 µg/mL, and CTX (128) + QUE (32); cefotaxime at 128 µg/mL plus quercetin at 32 µg/mL. Polymyxin B was used as a positive control. The values plotted are the means of 3 observations (n = 3). Data are expressed as mean ± S.D. Means that share the same superscript are not significantly different from each other (Tukey's HSD, $p < 0.05$).

Anti-biofilm formation

The inhibitory effects on biofilm formation of *A. baumannii* DMST 45378 after treatment with cefotaxime (CTX) and quercetin (QUE) individually and in combination at 24 and 48 h (**Figure 4**). The untreated control bacteria (CON) formed significant biofilm, as shown by the highest OD_{600} values. Single treatments with either CTX (512 µg/mL) or QUE (512 µg/mL) significantly reduced biofilm formation compared to controls. Notably, the combined sub-FIC treatment of CTX (128 µg/mL) plus QUE (32 µg/mL) showed the most pronounced anti-biofilm effect, significantly outperforming both single-agent treatments at 48 h ($p < 0.05$).

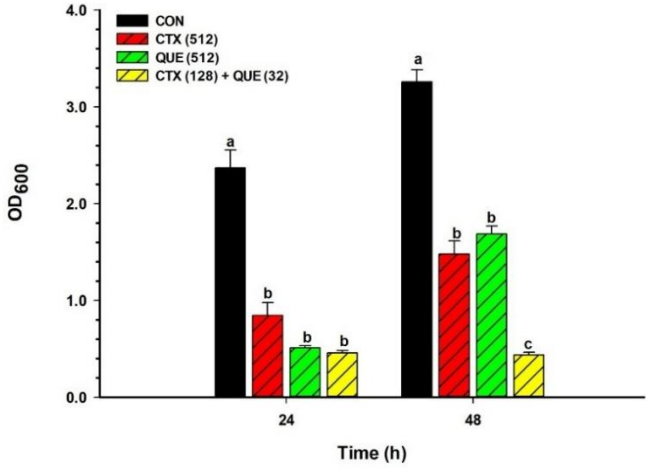


Figure 4 Anti-biofilm formation *A. baumannii* DMST 45378 after treatment with either sub-MIC of CTX or QUE alone and in combination at sub-FIC. CON; untreated control, CTX (512); cefotaxime at 512 µg/mL, QUE (512); quercetin at 512 µg/mL, and CTX (128) + QUE (32); cefotaxime at 128 µg/mL plus quercetin at 32 µg/mL. The values plotted are the means of 3 observations (n = 3). Data are expressed as mean ± S.D. Means sharing the same superscript are not significantly different from each other (Tukey's HSD, $p < 0.05$).

This highlights the synergistic potential of QUE combined with CTX in effectively preventing biofilm formation by *A. baumannii*. Biofilms contribute to virulence and antibiotic resistance [55]. While individual treatments modestly reduced biofilm formation, the CTX-QUE combination inhibited > 70%, likely through QUE's effects on adhesion, quorum sensing, and matrix disruption [56].

Scanning and transmission electron microscopes (SEM & TEM)

SEM analysis was employed to investigate alterations in cell morphology. Untreated *A. baumannii* DMST 45378 cells displayed intact morphology with smooth and uniform surfaces, indicating healthy bacterial cells (**Figure 5(A)**). Treatment with QUE at 512 µg/mL led to noticeable cell damage, characterized by abnormal morphology, cell membrane disruption (arrow with square tail), and irregular shapes (solid arrow), along with cell debris formation (arrow with star tail) (**Figure 5(B)**). CTX treatment at 512 µg/mL caused significant morphological disruptions, including elongated cell shapes (solid arrow), cell debris formation (arrow with star tail), and substantial cellular aggregation (**Figure 5(C)**). Remarkably, the combination of CTX (128 µg/mL) and QUE (32 µg/mL) resulted in extensive morphological deformities, exhibiting severe cell elongation (solid arrow), pronounced membrane damage (arrow with square tail), and considerable cell debris (arrow with star tail), representing more extensive cellular damage compared to either QUE or CTX alone (**Figure 5(D)**).

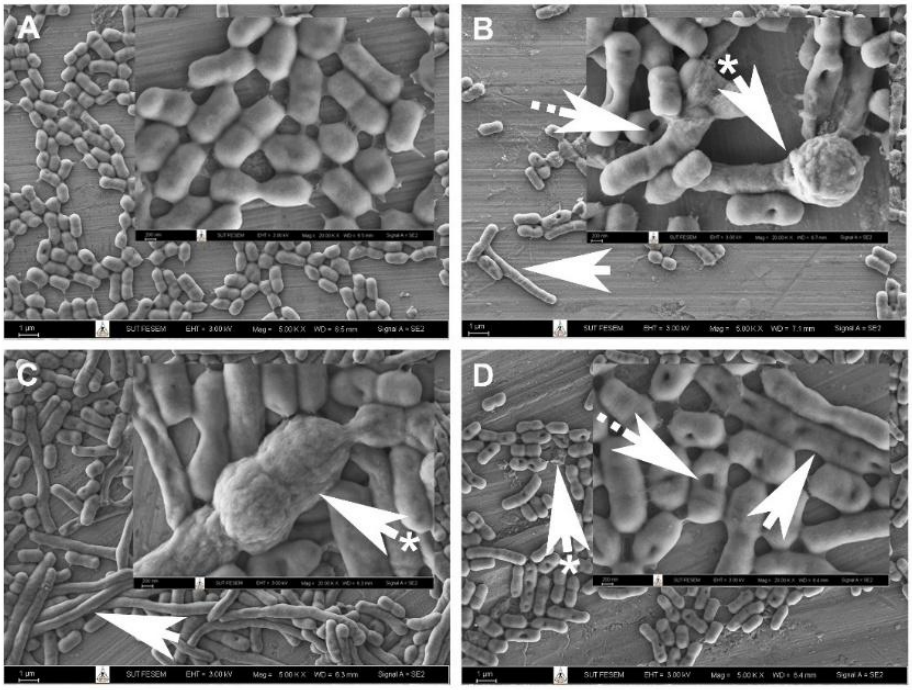


Figure 5 Scanning electron microscope images of untreated *A. baumannii* DMST 45378 (A), *A. baumannii* treated with QUE at 512 µg/mL (B), *A. baumannii* treated with CTX at 512 µg/mL (C), and *A. baumannii* treated with CTX at 128 µg/mL plus QUE at 32 µg/mL (D); (Magnification: A-D = 5,000×, bar = 1 µm; inset magnification: A-D = 20,000×, bar = 200 nm).

TEM analysis was conducted to examine ultrastructural changes within bacterial cells. Untreated *A. baumannii* DMST 45378 cells displayed intact cytoplasm and clearly defined cell envelopes, indicating healthy bacterial morphology (**Figure 6(A)**). Cells treated with QUE at 512 µg/mL showed moderate intracellular damage, including partial disruption of cytoplasmic density (arrow with square tail), and elongated cells (solid arrow) (**Figure 6(B)**). Treatment with CTX at 512 µg/mL resulted in substantial intracellular disturbances, characterized by noticeable cytoplasmic leakage (arrow with star tail) and elongated cell shapes (solid arrow) (**Figure 6(C)**). Remarkably, combined treatment with CTX (128 µg/mL) and QUE

(32 µg/mL) exhibited extensive and severe ultrastructural damage, including significant cytoplasmic content leakage (arrow with square tail), complete disruption and deformation of cell membranes (arrow with star tail), and pronounced intracellular irregularities, reflecting greater bacterial damage compared to either single agent alone (**Figure 6(D)**).

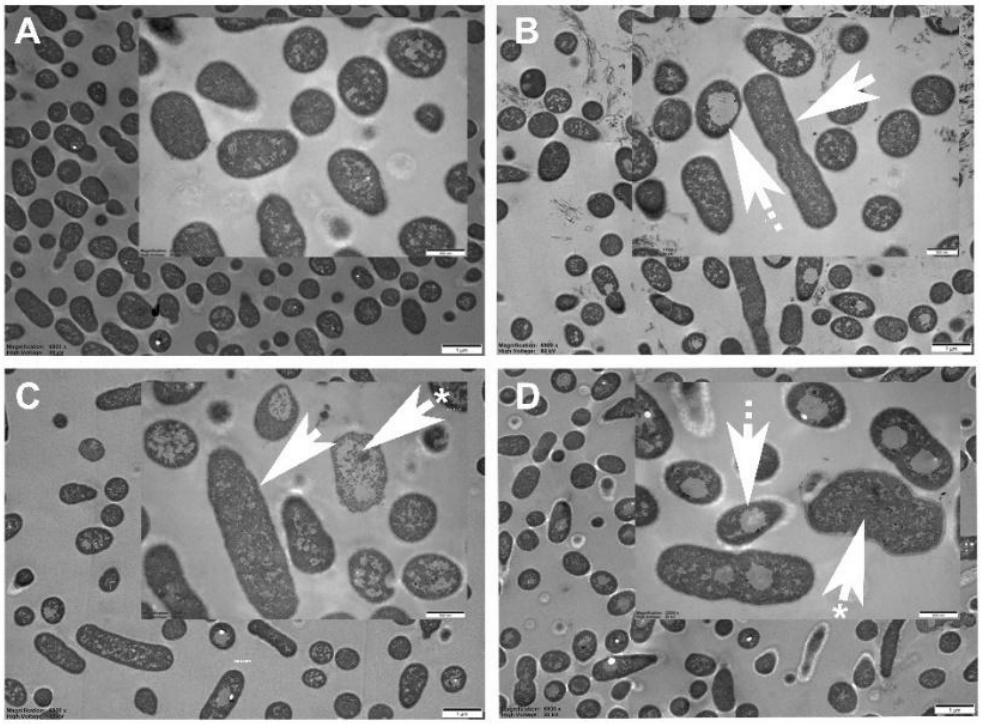


Figure 6 Transmission electron microscope images of untreated *A. baumannii* DMST 45378 (A), *A. baumannii* treated with QUE at 512 µg/mL (B), *A. baumannii* treated with CTX at 512 µg/mL (C), and *A. baumannii* treated with CTX at 128 µg/mL plus QUE at 32 µg/mL (D); (Magnification: A - D = 6,900×, bar = 1 µm; inset magnification: A, C, and D = 20,000×, B = 17,000×, bar = 500 nm).

Morphological and biochemical analyses corroborated these findings. SEM and TEM revealed moderate structural disruption with CTX or QUE alone, but severe damage, including membrane rupture and cytoplasmic leakage, with the combination [54,57,58]. This visual evidence strongly supports the synergistic mechanism of action, demonstrating how the combination profoundly compromises bacterial structure compared to either agent alone.

Fourier-transform infrared spectroscopy (FTIR)

The summary quantitative FTIR spectral analyzes by integrating key biochemical regions (lipids, proteins, nucleic acids, carbohydrates, and amide bands) in *A. baumannii* DMST 45378 after exposure to CTX, QUE, and their combination compared to untreated controls (CON) (**Figure 7**). Treatment significantly altered biochemical constituents: QUE treatment notably decreased integrated areas for lipids and carbohydrates, but increased protein and nucleic acids levels, compared to CTX and control ($p < 0.05$; **Figure 7(A)**). Similarly, amide I, II, and III bands were significantly affected by the QUE therapy, causing the most pronounced increase compared to CTX and control ($p < 0.05$; **Figure 7(B)**). Additionally, analysis of amide I/amide II ratios (**Figure 7(C)**) indicated substantial conformational changes in protein secondary structures, a significant decrease in the QUE group compared to other groups ($p < 0.05$).

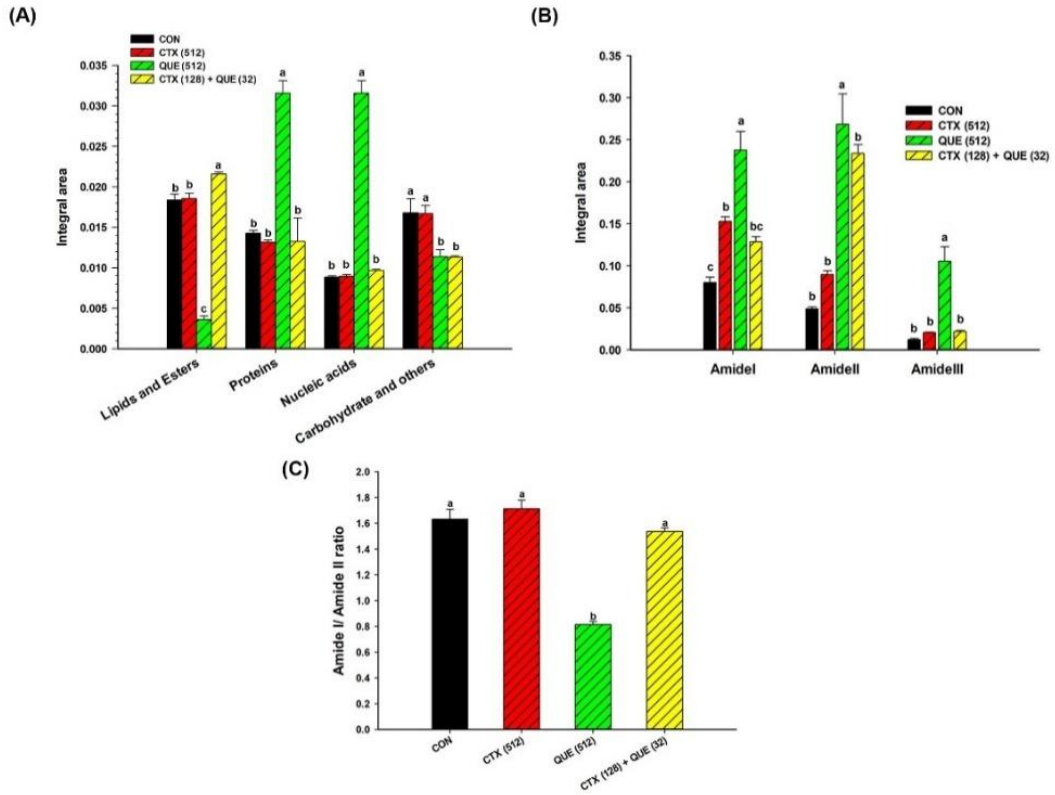


Figure 7 The integrated areas of remarkable lipid and esters, proteins, nucleic acids, carbohydrate, and other regions of *A. baumannii* DMST 45378. (A), the integrated area of protein derivatives (amide I, II, and III) (B), and the amide I/amide II ratio of 2nd derivative spectra (C). CON; untreated control, CTX (512); cefotaxime at 512 µg/mL, QUE (512); quercetin at 512 µg/mL, CTX (128) + QUE (32); cefotaxime at 128 µg/mL plus quercetin at 32 µg/mL. Data are represented as means ± S.D. in triplicate (n = 3). One-way ANOVA was performed for the comparison, and means sharing the same superscript are not significantly different from each other (Tukey's HSD, $p < 0.05$).

FTIR spectra confirmed these alterations, showing significant changes in lipid, carbohydrate, and protein regions, consistent with membrane destabilization, protein denaturation, and metabolic impairment [59,60]. The results may be inconsistent with the previous one that QUE can disrupt nucleic acid synthesis in both Gram-positive and Gram-negative bacteria by disturbing glycolytic, protein translation-elongation, and protein folding pathways [61,62].

Moreover, the integral area of the combination group suggests that a significant increase in lipid spectral regions underscores severe membrane disruptions, aligning closely with the morphological damage observed under electron microscopy. Furthermore, a decrease in carbohydrate spectral regions further suggests compromised bacterial cell-wall integrity or metabolic disruptions, reinforcing the notion of extensive cellular damage at the biochemical level and emphasizing the robust flavonoid-antibiotic synergistic action [63].

Cytotoxicity test

The cytotoxic effects of CTX and QUE, alone and in combination, were assessed using the MTT assay on cell viability. Cells were treated with varying concentrations of CTX (**Figure 8(A)**: 0 - 1,024 µg/mL) and QUE (**Figure 8(B)**: 0 - 1,024 µg/mL). The results demonstrated that CTX and QUE exhibited no significant cytotoxicity against HaCaT cells at concentrations up to 256 and 128 µg/mL, respectively, compared to negative (NA) and vehicle (VH) control groups ($p > 0.01$). The combination treatments (**Figure 8(C)**: CTX + QUE at 512 + 128, 256 + 64 and 128 + 32 µg/mL) also resulted in negligible cytotoxicity, maintaining viability close to untreated negative controls (NA) and vehicle (VH) control groups. Neither cefotaxime (CTX), quercetin (QUE), nor their

combination at antibacterial concentrations exhibited appreciable cytotoxicity under the tested *in vitro* conditions. Nonetheless, broader evaluation of safety and therapeutic applicability remains warranted.

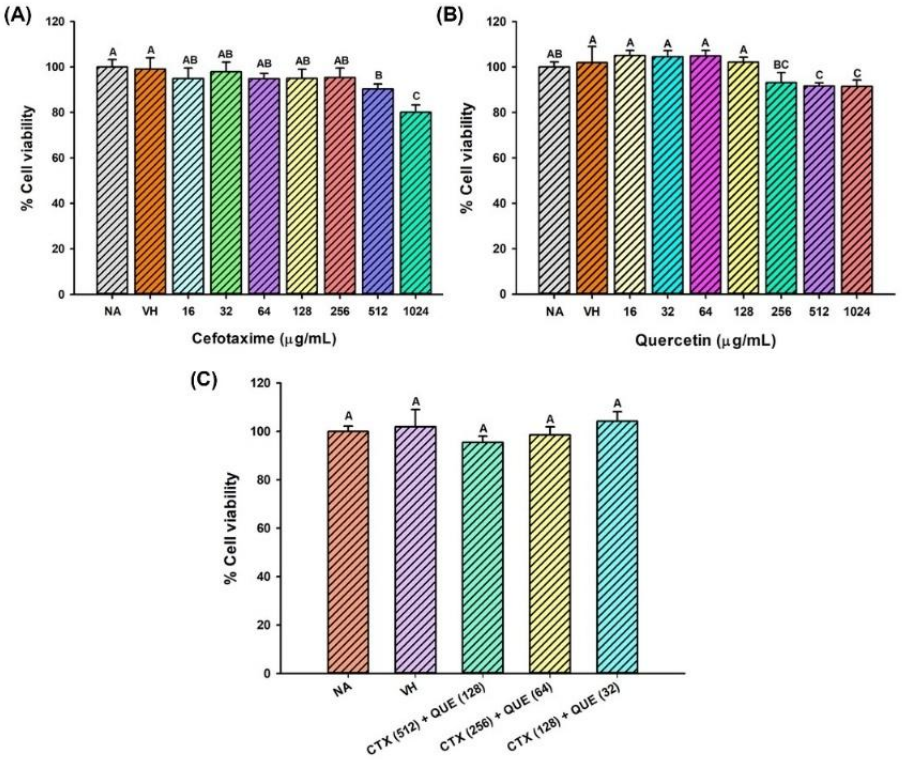


Figure 8 The cytotoxic effects of CTX and QUE, either individually or in combination, on HaCaT cells were evaluated using the MTT assay. HaCaT cells were treated with varying concentrations of cefotaxime (A) and quercetin (B), ranging from 0 to 1,024 µg/mL, and the combination of CTX and QUE at concentrations corresponding to the FICI values: 512 + 128, 256 + 64 and 128 + 32 µg/mL (C) for 24 h. Negative (NA) and vehicle (VH) controls consisted of cells in DMEM alone and cells in DMEM containing 0.2% (v/v) DMSO, respectively. Data are presented as the mean ± S.D. of triplicate (n = 3). Statistical comparisons were conducted using one-way ANOVA, with means sharing the same superscript considered not significantly different (LSD, $p < 0.01$).

Cytotoxicity assays on HaCaT cells demonstrated that CTX and QUE, alone or combined at ≤ 128 µg/mL, were non-toxic after 24 h. The combination even showed lower cytotoxicity compared to single agents, consistent with reports of QUE's low toxicity at concentrations up to 90 µg/mL, as well as studies confirming QUE's non-toxicity across a wide range from 3.0223 to 778 µg/mL [64,65]. Importantly, the synergistic combination of CTX and QUE showed reduced cytotoxicity compared to the agents used singly.

This study demonstrates that quercetin (QUE) potentiates the antibacterial activity of cefotaxime (CTX) against β-lactam-resistant *A. baumannii.* Synergy, confirmed by time kill assays and mechanistic analyses, underscores the novelty of combining a conventional β-lactam with a natural compound to counter resistance. Mechanistic investigations revealed that QUE enhances CTX efficacy through cell envelope disruption, inhibition of biofilm formation, and biomolecular alterations, while exhibiting no detectable cytotoxicity in human keratinocytes at the tested concentrations.

The findings indicate that natural compounds may restore or augment β-lactam activity, representing a potential adjunctive approach to combat multidrug resistance. Methodologically, the combined use of time kill assays, electron microscopy, and FTIR spectroscopy provided convergent evidence of synergy and mechanism, thereby enhancing the robustness of the results. However, the study was limited to 3 resistant strains, restricting generalizability. Detection of bla_{TEM} offered only preliminary evidence of β-lactamase-

mediated resistance, and additional mechanisms may underlie cefotaxime and imipenem resistance. Potential biases include strain selection and reliance on *in vitro* assays, which may not fully reflect clinical complexity.

Future studies should include larger and more diverse clinical isolates, investigate additional resistance determinants, and assess pharmacological, pharmacokinetic, *in vivo* efficacy, and safety. Addressing these aspects will strengthen scientific rigor and credibility, while clarifying the broader therapeutic potential of CTX–QUE combinations against WHO critical priority pathogens, particularly β-lactam-resistant *A. baumannii.*

Conclusions

This study demonstrates the strong synergistic activity of flavonoid–antibiotic combinations against multidrug-resistant pathogens, with pronounced efficacy against β-lactam-resistant *A. baumannii*. The synergy was mediated through complementary mechanisms, including disruption of the cell envelope and increased membrane permeability, leading to leakage of intracellular DNA, RNA, and enzymatic contents. Furthermore, these combinations markedly inhibited biofilm formation, underscoring their potential to address persistent and refractory infections. Importantly, *in vitro* cytotoxicity assays revealed minimal toxicity, supporting a favorable safety profile.

These findings provide compelling evidence that flavonoids can potentiate conventional antibiotics by disrupting bacterial cell integrity and interfering with essential biomolecular processes. Owing to their robust synergistic activity and low cytotoxicity, flavonoid–antibiotic combinations represent a promising adjunctive therapeutic strategy. This approach offers an innovative avenue to address infections caused by WHO critical priority pathogens, particularly β-lactam-resistant *A. baumannii*. Nonetheless, further studies are required to comprehensively assess efficacy, safety, and clinical applicability before these combinations can be advanced as viable adjunct therapies against WHO critical priority pathogens.

Acknowledgements

This work was supported by the Royal Golden Jubilee Ph. D. Program (Grant No. PHD/0097/2560). Additional support was provided by Suranaree University of Technology (SUT), Thailand Science Research and Innovation (TSRI), and the National Science, Research and Innovation Fund (NSRF). The authors also gratefully acknowledge the Synchrotron Light Research Institute (Nakhon Ratchasima, Thailand) for providing access to the light source at beamline 4.1 for FTIR analysis.

Declaration of generative AI in scientific writing

During the preparation of this manuscript, the authors utilized ChatGPT and Quillbot, AI-based writing assistants, to refine language and readability. Following the application of this tool/service, the authors thoroughly reviewed and edited the content as necessary and take full responsibility for the final published version.

CRediT author statement

Intu-orn Ayamuang: Conceptualization; Methodology; Validation; Formal analysis; Writing - Original Draft; Visualization. **Yothin Teethaisong**: Conceptualization; Methodology; Resources; Writing - Review & Editing. **Santi Watthana**: Supervision. **Kittipot Sirichaiwetchakoon**: Formal analysis; Resources. **Benjawan Dunkhunthod**: Resources; Methodology. **Siriporn Suknasang**: Methodology; Resources. **Yupaporn Chaiseha**: Funding acquisition. **Griangsak Eumkeb**: Supervision; Conceptualization; Resources; Writing - Review & Editing; Visualization; Funding acquisition.

References

[1] MR De Blasiis, A Sciurti, V Baccolini, C Isonne, M Ceparano, J Iera, C De Vito, C Marzuillo, P Villari and G Migliara. Impact of antibiotic exposure on antibiotic-resistant *Acinetobacter baumannii* isolation in intensive care unit patients: A systematic review and meta-analysis. *Journal of Hospital Infection* 2024; **143**, 123-139.

[2] GJ Da Silva and S Domingues. Insights on the horizontal gene transfer of carbapenemase determinants in the opportunistic pathogen *Acinetobacter baumannii*. *Microorganisms* 2016; **4(3)**, 29.

[3] C Dallenne, A Da Costa, D Decré, C Favier and G Arlet. Development of a set of multiplex PCR assays for the detection of genes encoding

important *β*-lactamases in Enterobacteriaceae. *Journal of Antimicrobial Chemotherapy* 2010; **65(3)**, 490-495.

[4] S Singh, S Singh, M Trivedi and M Dwivedi. An insight into MDR *Acinetobacter baumannii* infection and its pathogenesis: Potential therapeutic targets and challenges. *Microbial Pathogenesis* 2024; **192**, 106674.

[5] World Health Organization. *WHO bacterial priority pathogens list, 2024: Bacterial pathogens of public health importance to guide research, development and strategies to prevent and control antimicrobial resistance.* 2024, Available at: https://www.who.int/news/item/17-05-2024-who-updates-list-of-drug-resistant-bacteria-most-threatening-to-human-health, accessed April 2026.

[6] CR Lee, JH Lee, M Park, KS Park, IK Bae, YB Kim, CJ Cha, BC Jeong and SH Lee. Biology of *Acinetobacter baumannii*: Pathogenesis, antibiotic resistance mechanisms, and prospective treatment options. *Frontiers in Cellular and Infection Microbiology* 2017; **7**, 55.

[7] G Eumkeb, S Siriwong, S Phitaktim, N Rojtinnakorn and S Sakdarat. Synergistic activity and mode of action of flavonoids isolated from smaller galangal and amoxicillin combinations against amoxicillin-resistant *Escherichia coli*. *Journal of Applied Microbiology* 2012; **112(1)**, 55-64.

[8] S Phitaktim, M Chomnawang, K Sirichaiwetchakoon, B Dunkhunthod, G Hobbs and G Eumkeb. Synergism and the mechanism of action of the combination of α-mangostin isolated from *Garcinia mangostana* L. and oxacillin against an oxacillin-resistant *Staphylococcus saprophyticus*. *BMC Microbiology* 2016; **16(1)**, 195.

[9] SE Weinberg, A Villedieu, N Bagdasarian, N Karah, L Teare and WF Elamin. Control and management of multidrug resistant *Acinetobacter baumannii*: A review of the evidence and proposal of novel approaches. *Infection Prevention in Practice* 2020; **2(3)**, 100077.

[10] ED Wilkie, JO Alao and TA Akinmolayan. *Host-pathogen interactions in acinetobacter baumannii infections: Mechanisms of immune evasion and potential therapeutic targets. In*: K Rangel and S De Simone (Eds.). *Acinetobacter baumannii* - the rise of a resistant pathogen: The rise of a resistant pathogen. IntechOpen, London, 2024, p. 65-67.

[11] S Roy, G Chowdhury, AK Mukhopadhyay, S Dutta and S Basu. Convergence of biofilm formation and antibiotic resistance in *Acinetobacter baumannii* infection. *Frontiers in Medicine* 2022; **9**, 793615.

[12] TD Gootz. The global problem of antibiotic resistance. *Critical Reviews™ in Immunology* 2010; **30(1)**, 79-93.

[13] K Kengkla, K Kongpakwattana, S Saokaew, A Apisarnthanarak and N Chaiyakunapruk. Comparative efficacy and safety of treatment options for MDR and XDR *Acinetobacter baumannii* infections: A systematic review and network meta-analysis. *Journal of Antimicrobial Chemotherapy* 2018; **73(1)**, 22-32.

[14] PA Todd and RN Brogden. Cefotaxime: An update of its pharmacology and therapeutic use. *Drugs* 1990; **40(4)**, 608-651.

[15] National Drug Information. National list of essential medicines, Available at: https://ndi.fda.moph.go.th/drug_national, accessed April 2026.

[16] National Antimicrobial Resistant Surveillance Center. *Antimicrobial resistance antibiogram*, Available at: https://narst.dmsc.moph.go.th/antibiogram, accessed April 2026.

[17] K Bush and JF Fisher. Epidemiological expansion, structural studies, and clinical challenges of new *β*-lactamases from gram-negative bacteria. *Annual Review of Microbiology* 2011; **65**, 455-478.

[18] PJ Shah and MT Williamson. Evaluation of synergism between cefotaxime and *Allium sativum* against extended spectrum beta-lactamase and Ambler class C co-producers. *Journal of Applied Pharmaceutical Science* 2019; **9(03)**, 098-104.

[19] EM Halawani, AM Hassan and SMG El-Rab. Nanoformulation of biogenic cefotaxime-conjugated-silver nanoparticles for enhanced antibacterial efficacy against multidrug-resistant bacteria and anticancer studies. *International Journal of Nanomedicine* 2020; **15**, 1889.

[20] X Liu, L Ma, F Chen, J Liu, H Yang and Z Lu. Synergistic antibacterial mechanism of Bi_2Te_3 nanoparticles combined with the ineffective *β*-lactam antibiotic cefotaxime against methicillin-resistant *Staphylococcus aureus. Journal of Inorganic Biochemistry* 2019; **196**, 110687.

[21] B Muchtaromah, AM Firdaus, AN Ansori, MR Duhita, EB Minarno, A Hayati, M Ahmad and I Analisa. Effect of pegagan (*Centella asiatica*) nanoparticle coated with chitosan on the cytokine profile of chronic diabetic mice. *Narra J* 2024; **4(1)**, e697.

[22] H Padmi, VD Kharisma, ANM Ansori, MT Sibero, MH Widyananda, ME Ullah, O Gumenyuk, S Chylichcova, N Bratishko and ES Prasedya. Macroalgae bioactive compounds for the potential antiviral of SARS-CoV-2: An *in silico* study. *Journal of Pure and Applied Microbiology* 2022; **16(2)**, 1018-1027.

[23] MH Widyananda, SK Pratama, ANM Ansori, Y Antonius, VD Kharisma, AAA Murtadlo, V Jakhmola, M Rebezov, M Khayrullin and M Derkho. Quercetin as an anticancer candidate for glioblastoma multiforme by targeting AKT1, MMP9, ABCB1, and VEGFA: An *in silico* study. *Karbala International Journal of Modern Science* 2023; **9(3)**, 10.

[24] WC Rizky, MC Jihwaprani, A Kindi, ANM Ansori and M Mushtaq. The pharmacological mechanism of quercetin as adjuvant therapy of COVID-19. *Life Res*earch 2022; **5(3)**, 1-9.

[25] AM Hossion, Y Zamami, RK Kandahary, T Tsuchiya, W Ogawa, A Iwado and K Sasaki. Quercetin diacylglycoside analogues showing dual inhibition of DNA gyrase and topoisomerase IV as novel antibacterial agents. *Journal of Medicinal Chemistry* 2011; **54(11)**, 3686-3703.

[26] D Wu, Y Kong, C Han, J Chen, L Hu, H Jiang and X Shen. D-Alanine: D-alanine ligase as a new target for the flavonoids quercetin and apigenin. *International Journal of Antimicrobial Agents* 2008; **32(5)**, 421-426.

[27] K Ganesan and B Xu. A critical review on polyphenols and health benefits of black soybeans. *Nutrients* 2017; **9(5)**, 455.

[28] M Alvarez, N Debattista and N Pappano. Antimicrobial activity and synergism of some substituted flavonoids. *Folia Microbiologica* 2008; **53(1)**, 23-28.

[29] W Hertel, G Peschel, JH Ozegowski and PJ Müller. Inhibitory effects of triterpenes and flavonoids on the enzymatic activity of hyaluronic acid-splitting enzymes. *Archiv der Pharmazie: An International Journal Pharmaceutical and Medicinal Chemistry* 2006; **339(6)**, 313-318.

[30] S Siriwong, Y Teethaisong, K Thumanu, B Dunkhunthod and G Eumkeb. The synergy and mode of action of quercetin plus amoxicillin against amoxicillin-resistant *Staphylococcus epidermidis. BMC Pharmacology and Toxicology* 2016; **17(1)**, 39.

[31] F Geoghegan, R Wong and A Rabie. Inhibitory effect of quercetin on periodontal pathogens *in vitro. Phytotherapy Research* 2010; **24(6)**, 817-820.

[32] O Ustün, B Ozçelik, Y Akyön, U Abbasoglu and E Yesilada. Flavonoids with anti-*Helicobacter pylori* activity from *Cistus laurifolius* leaves. *Journal of Ethnopharmacology* 2006; **108(3)**, 457-461.

[33] Clinical Laboratory Standards Institute. *CLSI document M100*: *Performance standards for antimicrobial susceptibility testing.* 32nd ed. Clinical Laboratory Standards Institute, Philadelphia, United States, 2022.

[34] IX Liu, DG Durham and RME Richards. Baicalin synergy with *β*-lactam antibiotics against methicillin-resistant *Staphylococcus aureus* and other *β*-lactam-resistant strains of *S. aureus. Journal of Pharmacy and Pharmacology* 2000; **52(3)**, 361-366.

[35] FJ Pérez-Pérez and ND Hanson. Detection of plasmid-mediated AmpC *β*-lactamase genes in clinical isolates by using multiplex PCR. *Journal of Clinical Microbiology* 2002; **40(6)**, 2153-2162.

[36] Y Teethaisong, G Eumkeb, S Chumnarnsilpa, N Autarkool, J Hobson, I Nakouti, G Hobbs and K Evans. Phenotypic detection of AmpC *β*-lactamases, extended-spectrum *β*-lactamases and metallo-*β*-lactamases in Enterobacteriaceae using a resazurin microtitre assay with inhibitor-based methods. *Journal of Medical Microbiology* 2016; **65(10)**, 1079-1087.

[37] CR Bonapace, JA Bosso, LV Friedrich and RL White. Comparison of methods of interpretation of checkerboard synergy testing. *Diagnostic Microbiology and Infectious Disease* 2002; **44(4)**, 363-366.

[38] MB Marques, ES Brookings, SA Moser, PB Sonke and KB Waites. Comparative *in vitro* antimicrobial susceptibilities of nosocomial isolates of *Acinetobacter baumannii* and synergistic activities of nine antimicrobial combinations. *Antimicrobial Agents and Chemotherapy* 1997; **41(5)**, 881-885.

[39] R Michael, E Richards and DK Xing. *In vitro* evaluation of the antimicrobial activities of selected lozenges. *Journal of Pharmaceutical Sciences* 1993; **82(12)**, 1218-1220.

[40] Y Teethaisong, N Autarkool, K Sirichaiwetchakoon, P Krubphachaya, S Kupittayanant and G Eumkeb. Synergistic activity and mechanism of action of *Stephania suberosa* Forman extract and ampicillin combination against ampicillin-resistant *Staphylococcus aureus*. *Journal of Biomedical Science* 2014; **21(1)**, 90.

[41] R Gopal, YG Kim, JH Lee, SK Lee, JD Chae, BK Son, CH Seo and Y Park. Synergistic effects and antibiofilm properties of chimeric peptides against multidrug-resistant *Acinetobacter baumannii* strains. *Antimicrobial Agents and Chemotherapy* 2014; **58(3)**, 1622-1629.

[42] Y Teethaisong, T Pimchan, R Srisawat, G Hobbs and G Eumkeb. *Boesenbergia rotunda* (L.) Mansf. extract potentiates the antibacterial activity of some *β*-lactams against *β*-lactam-resistant staphylococci. *Journal of Global Antimicrobial Resistance* 2018; **12**, 207-213.

[43] HM Al-Qadiri, NI Al-Alami, MA Al-Holy and BA Rasco. Using Fourier transform infrared (FT-IR) absorbance spectroscopy and multivariate analysis to study the effect of chlorine-induced bacterial injury in water. *Journal of Agricultural and Food Chemistry* 2008; **56(19)**, 8992-8997.

[44] KP Devi, SA Nisha, R Sakthivel and SK Pandian. Eugenol (an essential oil of clove) acts as an antibacterial agent against *Salmonella typhi* by disrupting the cellular membrane. *Journal of Ethnopharmacology* 2010; **130(1)**, 107-115.

[45] B Dunkhunthod, C Talabnin, M Murphy, K Thumanu, P Sittisart and G Eumkeb. *Gymnema inodorum* (Lour.) Decne. extract alleviates oxidative stress and inflammatory mediators produced by RAW264. 7 macrophages. *Oxidative Medicine and Cellular Longevity* 2021; **2021(1)**, 8658314.

[46] LC Antunes, P Visca and KJ Towner. *Acinetobacter baumannii*: Evolution of a global pathogen. *Pathogens and Disease* 2014; **71(3)**, 292-301.

[47] GS Kogilathota Jagirdhar, K Rama, ST Reddy, H Pattnaik, RK Qasba, PR Elmati, R Kashyap, M Schito and N Gupta. Efficacy of cefoperazone sulbactam in patients with Acinetobacter infections: a systematic review of the literature. *Antibiotics* 2023; **12(3)**, 582.

[48] BA Evans and SG Amyes. OXA β-lactamases. *Clinical Microbiology Reviews* 2014; **27(2)**, 241-263.

[49] A Pal and A Tripathi. Quercetin potentiates meropenem activity among pathogenic carbapenem-resistant *Pseudomonas aeruginosa* and *Acinetobacter baumannii*. *Journal of Applied Microbiology* 2019; **127(4)**, 1038-1047.

[50] S Ghafourian, N Sadeghifard, S Soheili and Z Sekawi. Extended spectrum beta-lactamases: definition, classification and epidemiology. *Current Issues in Molecular Biology* 2015; **17(1)**, 11-22.

[51] DL Paterson and RA Bonomo. Extended-spectrum *β*-lactamases: A clinical update. *Clinical Microbiology Reviews* 2005; **18(4)**, 657-686.

[52] AY Peleg, H Seifert and DL Paterson. *Acinetobacter baumannii*: Emergence of a successful pathogen. *Clinical Microbiology Reviews* 2008; **21(3)**, 538-582.

[53] MJ Trimble, P Mlynárčik, M Kolář and RE Hancock. Polymyxin: alternative mechanisms of action and resistance. *Cold Spring Harbor Perspectives in Medicine* 2016; **6(10)**, a025288.

[54] TT Cushnie and AJ Lamb. Recent advances in understanding the antibacterial properties of flavonoids. *International Journal of Antimicrobial Agents* 2011; **38(2)**, 99-107.

[55] CW Hall and TF Mah. Molecular mechanisms of biofilm-based antibiotic resistance and tolerance

in pathogenic bacteria. *FEMS Microbiology Reviews* 2017; **41(3)**, 276-301.

[56] IASV Packiavathy, P Sasikumar, SK Pandian and A Veera Ravi. Prevention of quorum-sensing-mediated biofilm development and virulence factors production in *Vibrio spp.* by curcumin. *Applied Microbiology and Biotechnology* 2013; **97**, 10177-10187.

[57] LB Chibane, V Forquet, P Lantéri, Y Clément, LL Akkari, N Oulahal, P Degraeve and C Bordes. Antibacterial properties of polyphenols: Characterization and QSAR (Quantitative structure-activity relationship) models. *Frontiers in Microbiology* 2019; **10**, 829.

[58] T Guo, M Li, X Sun, Y Wang, L Yang, H Jiao and G Li. Synergistic activity of capsaicin and colistin against colistin-resistant *Acinetobacter baumannii*: *In vitro*/*vivo* efficacy and mode of action. *Frontiers in Pharmacology* 2021; **12**, 744494.

[59] D Naumann. Infrared spectroscopy in microbiology. *Encyclopedia of Analytical Chemistry* 2000; **102**, 131.

[60] Â Novais, AR Freitas, C Rodrigues and L Peixe. Fourier transform infrared spectroscopy: Unlocking fundamentals and prospects for bacterial strain typing. *European Journal of Clinical Microbiology & Infectious Diseases* 2019; **38**, 427-448.

[61] TLA Nguyen and D Bhattacharya. Antimicrobial activity of quercetin: An approach to its mechanistic principle. *Molecules* 2022; **27(8)**, 2494.

[62] S Qayyum, D Sharma, D Bisht and AU Khan. Identification of factors involved in *Enterococcus faecalis* biofilm under quercetin stress. *Microbial Pathogenesis* 2019; **126**, 205-211.

[63] K Maquelin, LPC Smith, C Kirschner, NN Thi, D Naumann and G Puppels. *Vibrational spectroscopic studies of microorganisms.In*: P Griffiths and JM Chalmers (Eds.). Handbook of vibrational spectroscopy. John Wiley & Sons, New Jersey, United States, 2006.

[64] M Kalinowska, H Lewandowska, M Pruszyński, G Świderski, E Gołębiewska, K Gryko, J Braun, M Borkowska, M Konieczna and W Lewandowski. Co (II) complex of quercetin-spectral, anti-/pro-oxidant and cytotoxic activity in HaCaT cell lines. *Applied Sciences* 2021; **11(19)**, 9244.

[65] SY Seo, WS Ju, K Kim, J Kim, JO Yu, JS Ryu, JS Kim, HA Lee, DB Koo and YK Choo. Quercetin induces mitochondrial apoptosis and downregulates ganglioside GD3 expression in melanoma cells. *International Journal of Molecular Sciences* 2024; **25(10)**, 5146.

Supplementary Materials

Table S1 Primer sequences for detection of *bla*$_{ampC}$ family genes [32].

Target Genes	Sequences (5′→3′)	Primer concentration (μM)	Product Size (bp)
bla$_{MOXM}$ (F)	GCT GCT CAA GGA GCA CAG GAT	0.5	520
bla$_{MOXM}$ (R)	CAC ATT GAC ATA GGT GTG GTG C	0.5	
bla$_{CITM}$ (F)	TGG CCA GAA CTG ACA GGC AAA	0.5	462
bla$_{CITM}$ (R)	TTT CTC CTG AAC GTG GCT GGC	0.5	
bla$_{DHAM}$ (F)	AAC TTT CAC AGG TGT GCT GGG T	0.5	405
bla$_{DHAM}$ (R)	CCG TAC GCA TAC TGG CTT TGC	0.5	
bla$_{ACCM}$ (F)	AAC AGC CTC AGC AGC CGG TTA	0.5	346
bla$_{ACCM}$ (R)	TTC GCC GCA ATC ATC CCT AGC	0.5	
bla$_{EBCM}$ (F)	TCG GTA AAG CCG ATG TTG CGG	0.5	302
bla$_{EBCM}$ (R)	CTT CCA CTG CGG CTG CCA GTT	0.5	
bla$_{FOX-M}$ (F)	AAC ATG GGG TAT CAG GGA GAT G	0.5	190
bla$_{FOX-M}$ (R)	CAA AGC GCG TAA CCG GAT TGG	0.5	

Table S2 Primer sequences for detection of *bla*$_{ESBL}$ family genes [3].

Target Genes	Sequences (5′→3′)	Primer concentration (μM)	Product Size (bp)
Multiplex I			
bla$_{TEM}$ (F)	CAT TTC CGT GTC GCC CTT ATT C	0.5	800
bla$_{TEM}$ (R)	CGT TCA TCC ATA GTT GCC TGA C	0.5	
bla$_{SHV}$ (F)	AGC CGC TTG AGC AAA TTA AAC	0.5	713
bla$_{SHV}$ (R)	ATC CCG CAG ATA AAT CAC CAC	0.5	
Multiplex II			
bla$_{CTX-M\ group\ 1}$ (F)	TTA GGA ART GTG CCG CTG YA[a]	0.5	688
bla$_{CTX-M\ group\ 1}$ (R)	CGA TAT CGT TGG TGG TRC CAT[a]	0.5	
bla$_{CTX-M\ group\ 2}$ (F)	CGT TAA CGG CAC GAT GAC	0.5	404
bla$_{CTX-M\ group\ 2}$ (R)	CGA TAT CGT TGG TGG TRC CAT[a]	0.5	
bla$_{CTX-M\ group\ 9}$ (F)	TCA AGC CTG CCG ATC TGG T	0.5	561
bla$_{CTX-M\ group\ 9}$ (R)	TGA TTC TCG CCG CTG AAG	0.5	
bla$_{CTX-M\ group\ 8/15}$ (F)	AAC RCR CAG ACG CTC TAC[a]	0.5	326
bla$_{CTX-M\ group\ 8/15}$ (R)	TCG AGC CGG AAS GTG TYA T[a]	0.5	

[a] = Y = T or C; R = A or G; S = G or C.

Table S3 Primer sequences for detection of *carbapenemase* family genes [3].

Target Genes	Sequences (5′→3′)	Primer concentration (μM)	Product Size (bp)
bla$_{\text{NDM-type}}$ (F)	CCT CAA CTG GAT CAA GCA GG	0.4	341
bla$_{\text{NDM-type}}$ (R)	CCT TGC TGT CCT TGA TCA GG	0.4	
bla$_{\text{KPC-type}}$ (F)	CAT TCA AGG GCT TTC TTG CTG C	0.4	538
bla$_{\text{KPC-type}}$ (R)	ACG ACG GCA TAG TCA TTT GC	0.4	
bla$_{\text{VIM-type}}$ (F)	GAT GGT GTT TGG TCG CAT A	0.5	390
bla$_{\text{VIM-type}}$ (R)	CGA ATG CGC AGC ACC AG	0.5	
bla$_{\text{OXA-48-like}}$ (F)	GCT TGA TCG CCC TCG ATT	0.6	281
bla$_{\text{OXA-48-like}}$ (R)	GAT TTG CTC CGT GGC CGA AA	0.6	
bla$_{\text{IMP-type}}$ (F)	TTG ACA CTC CAT TTA CDG[a]	0.6	139
bla$_{\text{IMP-type}}$ (R)	GAT YGA GAA TTA AGC CAC YCT[a]	0.6	

[a] = Y = T or C; D = A or G or T.